



Title	Optimization and evaluation of multiple gating beam delivery in a synchrotron-based proton beam scanning system using a real-time imaging technique
Author(s)	Yamada, Takahiro; Miyamoto, Naoki; Matsuura, Taeko; Takao, Seishin; Fujii, Yusuke; Matsuzaki, Yuka; Koyano, Hidenori; Umezawa, Masumi; Nihongi, Hideaki; Shimizu, Shinichi; Shirato, Hiroki; Umegaki, Kikuo
Citation	Physica medica : European journal of medical physics, 32(7), 932-937 <a href="https://doi.org/10.1016/j.ejmp.2016.06.002">https://doi.org/10.1016/j.ejmp.2016.06.002</a>
Issue Date	2016-07
Doc URL	<a href="http://hdl.handle.net/2115/66410">http://hdl.handle.net/2115/66410</a>
Rights	© 2016. This manuscript version is made available under the CC-BY-NC-ND 4.0 license <a href="http://creativecommons.org/licenses/by-nc-nd/4.0/">http://creativecommons.org/licenses/by-nc-nd/4.0/</a>
Rights(URL)	<a href="http://creativecommons.org/licenses/by-nc-nd/4.0/">http://creativecommons.org/licenses/by-nc-nd/4.0/</a>
Type	article (author version)
File Information	PhysicaMedica32_932.pdf



[Instructions for use](#)

# Optimization and evaluation of multiple gating beam delivery in a synchrotron-based proton beam scanning system using a real-time imaging technique

Takahiro Yamada <sup>a,c</sup>, Naoki Miyamoto <sup>a,\*</sup>, Taeko Matsuura <sup>d</sup>, Seishin Takao <sup>a</sup>, Yusuke Fujii <sup>a</sup>, Yuka Matsuzaki <sup>a</sup>, Hidenori Koyano <sup>b</sup>, Masumi Umezawa <sup>e</sup>, Hideaki Nihongi <sup>e</sup>, Shinichi Shimizu <sup>a,c</sup>, Hiroki Shirato <sup>a,c</sup>, Kikuo Umegaki <sup>a,c,d</sup>

<sup>a</sup> Proton Beam Therapy Center, Hokkaido University Hospital, North14 West5, Kita-ku, Sapporo, Hokkaido, 060-8638, Japan

<sup>b</sup> Department of Medical Physics, Graduate School of Medicine, Hokkaido University, North15 West7, Kita-ku, Sapporo, Hokkaido, 060-8638, Japan

<sup>c</sup> Global Station of Quantum Medical Science and Engineering, Global Institution for Collaborative Research and Education, Hokkaido University, North15 West7, Kita-ku, Sapporo, Hokkaido, 060-8638, Japan

<sup>d</sup> Division of Quantum Science and Engineering, Faculty of Engineering, Hokkaido University, North13 West8, Kita-ku, Sapporo, Hokkaido, 060-8638, Japan

<sup>e</sup> Hitachi Ltd. 1-1 7-chome, Oomika-cho, Hitachi-shi, Ibaraki, 319-1292, Japan

\* Corresponding author. Proton Beam Therapy Center, Hokkaido University Hospital, North14 West5, Kita-ku, Sapporo, Hokkaido, 060-8638, Japan. Tel.: +81 11 706 7638

E-mail address: [miya-nao@med.hokudai.ac.jp](mailto:miya-nao@med.hokudai.ac.jp) (Naoki Miyamoto)

**Purpose:**

To find the optimum parameter of a new beam control function installed in a synchrotron-based proton therapy system.

**Methods:**

A function enabling multiple gated irradiation in the flat top phase has been installed in a real-time-image gated proton beam therapy (RGPT) system. This function is realized by a waiting timer that monitors the elapsed time from the last gate-off signal in the flat top phase. The gated irradiation efficiency depends on the timer value,  $T_w$ . To find the optimum  $T_w$  value, gated irradiation efficiency was evaluated for each configurable  $T_w$  value. 271 gate signal data sets from 58 patients were used for the simulation.

**Results:**

The highest mean efficiency 0.52 was obtained in  $T_w = 0.2$  s. The irradiation efficiency was approximately 21% higher than at  $T_w = 0$  s, which corresponds to ordinary synchrotron operation. The irradiation efficiency was improved in 154 (57%) of the 271 cases. The irradiation efficiency was reduced in 117 cases because the  $T_w$  value was insufficient or the function introduced an unutilized wait time for the next gate-on signal in the flat top phase. In the actual treatment of a patient with a hepatic tumor at  $T_w = 0.2$  s, 4.48 GyE irradiation was completed within 250 s. In contrast, the treatment time of ordinary synchrotron operation was estimated to be 420 s.

**Conclusions:**

The results suggest that the multiple gated-irradiation function has potential to improve the gated irradiation efficiency and to reduce the treatment time.

**Keyword:** tumor tracking, spot scanning, respiratory motion, gated irradiation

## **Introduction**

Increasing numbers of proton therapy centers have adopted the spot-scanning technique. Spot scanning can potentially increase conformity to the target volume and modulates the dose more flexibly than the passive scattering approach. However, in beam scanning, the dose distribution may deteriorate under organ motions, such as respiratory or cardiac motions, during beam delivery [1-4]. Real-time four-dimensional radiotherapy, which includes beam gating [5-7] and beam tracking [8,9], has been realized in photon therapy to mitigate the dosimetric impacts of target motion. Gating [10-12] and tracking techniques [13,14] using external surrogates have also been reported in particle therapy. However, internal organ motions and the external surrogate signals of abdominal motion are not necessarily correlated during treatment [15]. Gated irradiation using internal fiducial markers based on real-time imaging is one of the best solutions in particle therapy.

In respiratory gated radiotherapy, reasonable gated irradiation efficiency is expected for clinical application. In carbon ion therapy system at National Institute of Radiological Science (NIRS), fast scanning technique including multi-energy irradiation with extended flat tops [16] and phase-controlled rescanning method [17] were realized to treat the mobile targets. By applying these techniques, reasonable treatment time can be achievable in NIRS carbon ion therapy. On the other hand, in the synchrotron for typical proton therapy system, beam current is relatively small compared with the carbon ion therapy system. In order to improve the gated irradiation efficiency with synchrotron based proton therapy, variable flat top phase synchrotron operation, described in the later section, has been applied. However, the gating signals change irregularly and sporadically under complex tumor motions [18] and, in some cases, poor recognition of the fiducial markers [19,20]. The resulting fluctuations in the gating signal can significantly reduce the gated irradiation efficiency in variable flat top phase synchrotron operation [21]. To improve the gated irradiation efficiency, we have developed a real-time-image gated proton beam therapy (RGPT) system [22-24] which has a new function, called the multiple gated-irradiation function [20,25]. The combination of variable flat top phase operation and multiple gated-irradiation function was realized in the first in RGPT. This

technique is the new approach to improve the gated irradiation efficiency.

Since the gated irradiation efficiency depends on the wait time  $T_w$  in multiple gated-irradiation function, we need to optimize this setting. As an initial step to use this new control function, we have decided to start RGPT with fixed  $T_w$  operation to make the treatment procedure simple. The purpose of this study is to evaluate the efficiency of gated irradiation and to find the optimum  $T_w$  which can improve the mean efficiency on the average.

## Materials and Methods

### *Real-time-image gated proton beam therapy (RGPT) system*

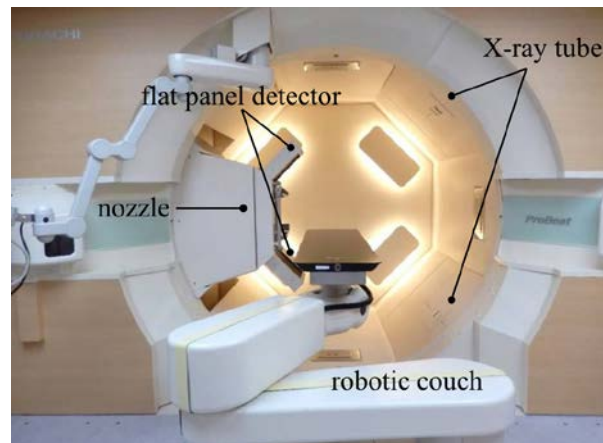


Figure 1. Overview of the real-time-image gated proton beam therapy (RGPT) system.

Figure 1 shows the RGPT system using a synchrotron-based accelerator. As indicated in the figure, a proton scanning nozzle, flat panel detectors, and X-ray tubes are installed in a rotating gantry. The real-time imaging system tracks the internal fiducial markers similarly to photon therapy and is based on the same concept [5]. The three-dimensional position of a fiducial marker located near the tumor is calculated from two fluoroscopic images obtained from orthogonal directions. The field of view is sized  $21.6 \text{ cm} \times 21.6 \text{ cm}$  at the isocenter plane. The image acquisition rate can be selected from discrete values ranging from 0.1 to 30 Hz. When the coordinates of the internal fiducial marker are within the gating window predefined in the treatment planning, the gate-on signal is transmitted from

the real-time imaging equipment to the beam irradiation controls. The typical size of the gating window in three directions (right-left, antero-posterior, and cranio-caudal) is  $\pm 2$  mm.

#### *Function of multiple gated irradiation*

The basic operation cycle of a synchrotron comprises an acceleration phase, a deceleration phase, and a flat top phase. In conventional operation, these phases are repeated at fixed durations. Unwanted synchronizations of the respiratory/cardiac motions and synchrotron operation pattern can degrade the efficiency of the respiratory-gated irradiation [25]. To improve the gated irradiation efficiency, a function enabling variable flat top phases has been reported [10]. The variable flat top phase operation has two characteristic functions: the first function waits for the first gate-on signal while maintaining the beam energy after the acceleration phase; the second decelerates the protons after gate-off during the flat top phase. In this way, unwanted synchronization of respiratory/cardiac motion and synchrotron operation can be avoided. However, the gate signals based on the internal markers are sensitive to slight changes in the identified marker positions near the gate boundaries, as shown in Fig. 2. In this case, the synchrotron decelerates the protons before they can be extracted in sufficient numbers due to frequent changes of the gate signals.

To improve the irradiation efficiency of the above gating technique, we have developed a novel function that enables multiple gated irradiations in the flat top phase [21,22]. This function is realized by a waiting timer that monitors the time elapsed since the previous gate-off signal in the flat top phase. As shown in Fig. 2, the beam irradiation can be promptly restarted without deceleration when the elapsed wait time is shorter than the predefined limit time ( $T_w$ ). The gated irradiation efficiency can be improved by applying this function.

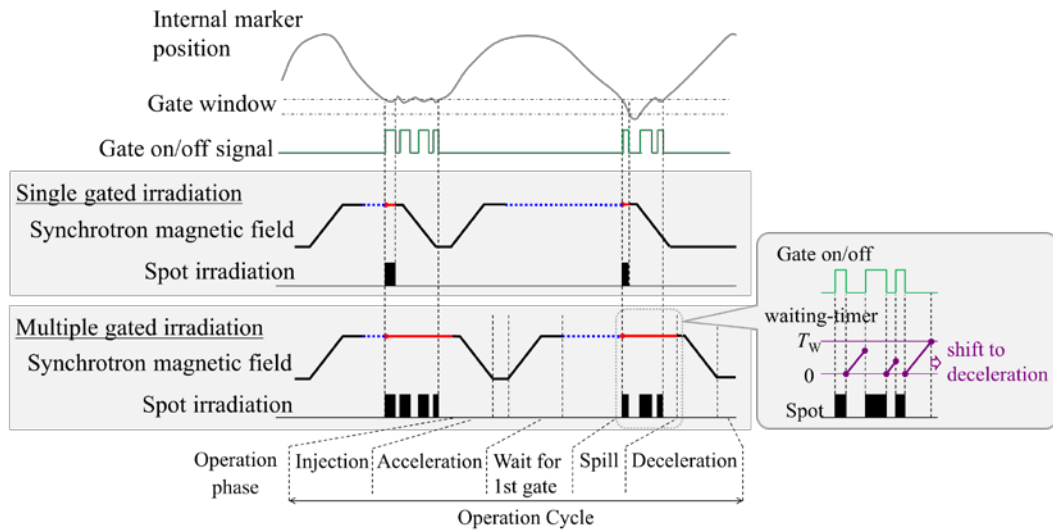


Figure 2. Comparison of synchrotron operation patterns in RGPT and single gated irradiation with variable flat top phases and multiple gated irradiation.

### *Evaluation of the gated irradiation efficiency*

The gated irradiation efficiency will depend on the  $T_w$  value. Beam irradiation profiles at typical  $T_w$  values are shown in Fig. 3. In this example, the efficiency of the multiple gated irradiation is higher at  $T_w$  of 0.2 and 0.5 s than at  $T_w = 0.0$  s but is reduced at  $T_w = 1.0$  s because of unutilized wait times. Hence, the optimum  $T_w$  should be identified prior to starting the RGPT. Therefore, we varied the  $T_w$  value and evaluated the gated irradiation efficiency by simulating the actual time-series data of the gate signals obtained from a photon real-time tumor-tracking radiotherapy (RTRT) system. The evaluation is detailed below.

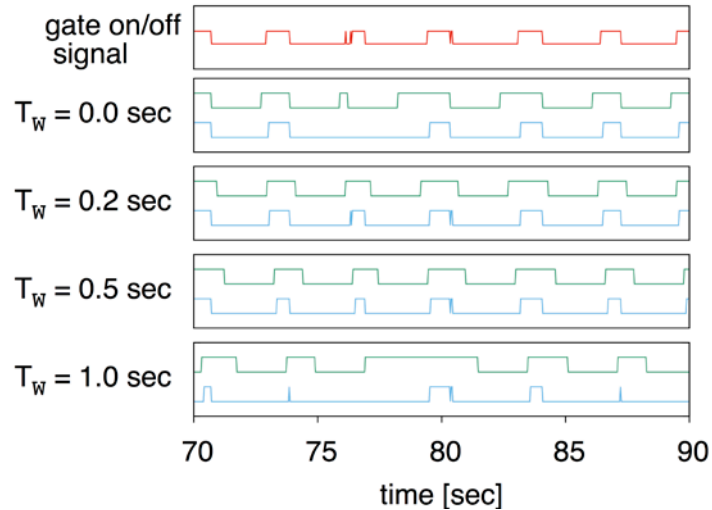


Figure 3. Examples of beam irradiation at different values of  $T_w$ . The upper signal and the lower signal in each  $T_w$  graph are synchrotron state and beam irradiation state respectively. High and low states of the synchrotron pattern represent the flat top and the deceleration/acceleration phases respectively.

*Clinical data of gate signals for the evaluation.*

The RTRT system records a log during X-ray fluoroscopy in the treatment session. The log file includes three-dimensional marker positions and the status of the gate signal (gate-on/gate-off) at 33 ms intervals. The log files for the evaluation were randomly chosen from lung cancer patients previously treated by photon RTRT. Some of the datasets included unidentified spike artifacts caused by unusual tumor motions such as coughing. These datasets were discarded. To simulate the usual beam gating conditions, log data with motion ranges less than 5 mm were also discarded. One dataset per patient was randomly chosen from one treatment day. Consequently, the evaluation dataset contained 271 gate signal data from 58 patients. The number of datasets per patient ranged from 1 to 25 (median = 4). Data collection times were  $125 \pm 81$  s (range 30–492 s), and the duty cycle of the gated irradiation, defined as the ratio of beam-on frames to the total frames, was  $0.51 \pm 0.18$  (range 0.11–0.98). Duty cycles were relatively large with small motions of the internal marker, as previously reported [26].

*Synchrotron operation parameters for the evaluation.*

The synchrotron operation parameters in the simulation were fixed to those of the current working system. The maximum flat top time ( $T_{FT}$ ) was 5.0 s, the maximum time of beam irradiation per cycle ( $T_{SP}$ ) was 3.8 s, and the total time of acceleration, deceleration, and injection was 2.0 s.

*Gated irradiation efficiency.*

The gated irradiation efficiency was evaluated by software developed in-house. The log data of the gate signals are imported, and the synchrotron operation cycle is simulated at predefined  $T_W$  values. The software counts the frame numbers of beam irradiation and the gate-on signal state in the log data. The gated irradiation efficiency  $E(T_W)$  for each  $T_W$  is defined as

$$E(T_W) = \frac{N_I(T_W)}{N_G}, \quad (1)$$

where  $N_I(T_W)$  and  $N_G$  are the frame numbers of the proton irradiation and gate-on, respectively.

The effect of starting phase is negligible in a synchrotron operated with a variable length flat top phase [10]. Therefore, in the evaluation, the start phase of the synchrotron was set to the acceleration phase. The  $T_W$  value that maximizes the irradiation efficiency will minimize the treatment time. We also investigated the treatment time of the first patient treated by RGPT.

## **Results**

Figure 4 shows the irradiation efficiency  $E(T_W)$  at each  $T_W$  determined from the 271 log datasets. The mean  $E(T_W)$  was maximized at 0.52 for  $T_W = 0.2$  s and was not improved by further increases in  $T_W$ . The maximum mean irradiation efficiency was approximately 21% higher than at  $T_W = 0$  s, which corresponds to ordinary synchrotron operation. By applying multiple gated irradiation with  $T_W = 0.2$  s, the irradiation efficiency was improved in 154 (57%) of the 271 cases. In contrast, the irradiation

efficiency was reduced in 117 cases because the  $T_w$  value was insufficient or the function introduced an unutilized wait time for the next gate-on signal in the flat top phase.

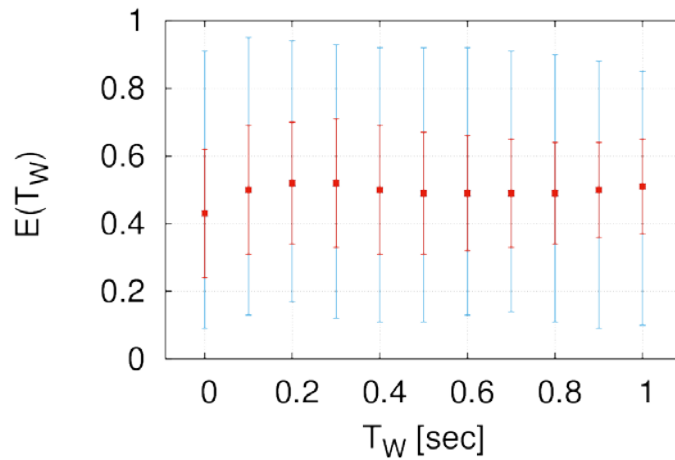


Figure 4. Gated irradiation efficiency for various values of  $T_w$ . Each point represents the mean efficiency of the 271 log datasets. Short (red) and long (blue) error bars represent the standard deviation and the range (minimum and maximum values), respectively.

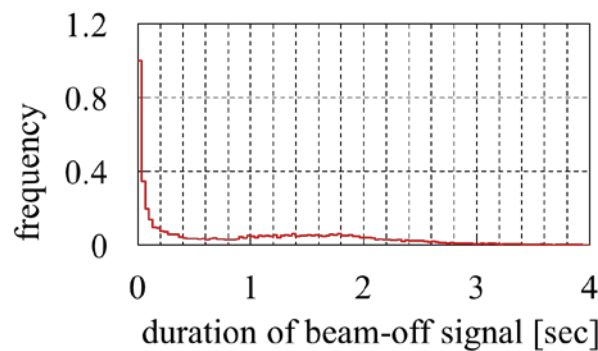


Figure 5. Normalized frequency histogram of the gate-off signal durations in the 271 log datasets.

The gated irradiation efficiency depends on the duration and frequency of the gate-off signal during treatment. Figure 5 is a normalized frequency histogram of the gate-off signal durations in the 271 log datasets. From 1 to 2 s, the beam is turned off by the respiratory motion cycle. The main distribution peak appears within 0.2 s, indicating frequent changes of the gate signals. This was one of the reasons why the mean irradiation efficiency was highest at  $T_w = 0.2$  s. As an initial step, we have started RGPT for cancer patients with  $T_w$  fixed at 0.2 s in the clinical setting.

For a detailed analysis, we investigated the relationship between  $T_W$  and the motion patterns of the internal fiducial marker. Fig. 6(a) and 6(b) show the normalized frequency histograms of the gate-off time for two patients. For Patient A, the main peaks vary from 0.1 s to 0.3 s (Fig. 6(a)), and  $T_W$  value exceeding 0.2 s would have been more appropriate. The high peaks for Patient B are distributed below 0.1 s (Fig. 6(b)), and so for this patient, the ideal  $T_W$  is shorter than 0.1 s. The time-series data of the gate signals of patients A and B are shown in Fig. 6(c) and 6(d), respectively. In both cases, the gate signals not only respond to the respiratory cycle but also exhibit frequent additional changes. The gate signal patterns differ between the patients because the motions of the internal fiducial marker are unique in each patient. The gate signals change frequently in Patient A since the fiducial marker was located near the heart. In this case, the marker trajectory includes both respiratory and cardiac motions, as shown in Fig. 6(e), and the gate signal would reflect this pattern of frequent motion. In Patient B, the gate signals respond to frequent slight changes in the identified marker position near the gate boundaries, as shown in Fig. 6(f). Thus, the optimum  $T_W$  value depends on the motion patterns of the internal fiducial marker.

To investigate the relationship between  $T_W$  and actual treatment time, the expected treatment times at various  $T_W$  values were investigated in one patient with a hepatic tumor who had been treated with RGPT. The treatment parameters were set as follows: Delivered dose = 4.48 GyE; number of energy layers = 21; energy range = 117.7–152.4 MeV; spot number in each layer was 3–346 (total spot number = 2270). The relative biological effectiveness was 1.1. The evaluation result is shown in Fig. 7. In the actual treatment, irradiation was completed within 250 s at  $T_W = 0.2$  s. Without multiple gated irradiation ( $T_W = 0$  s), the treatment time would have been prolonged to approximately 420 s.

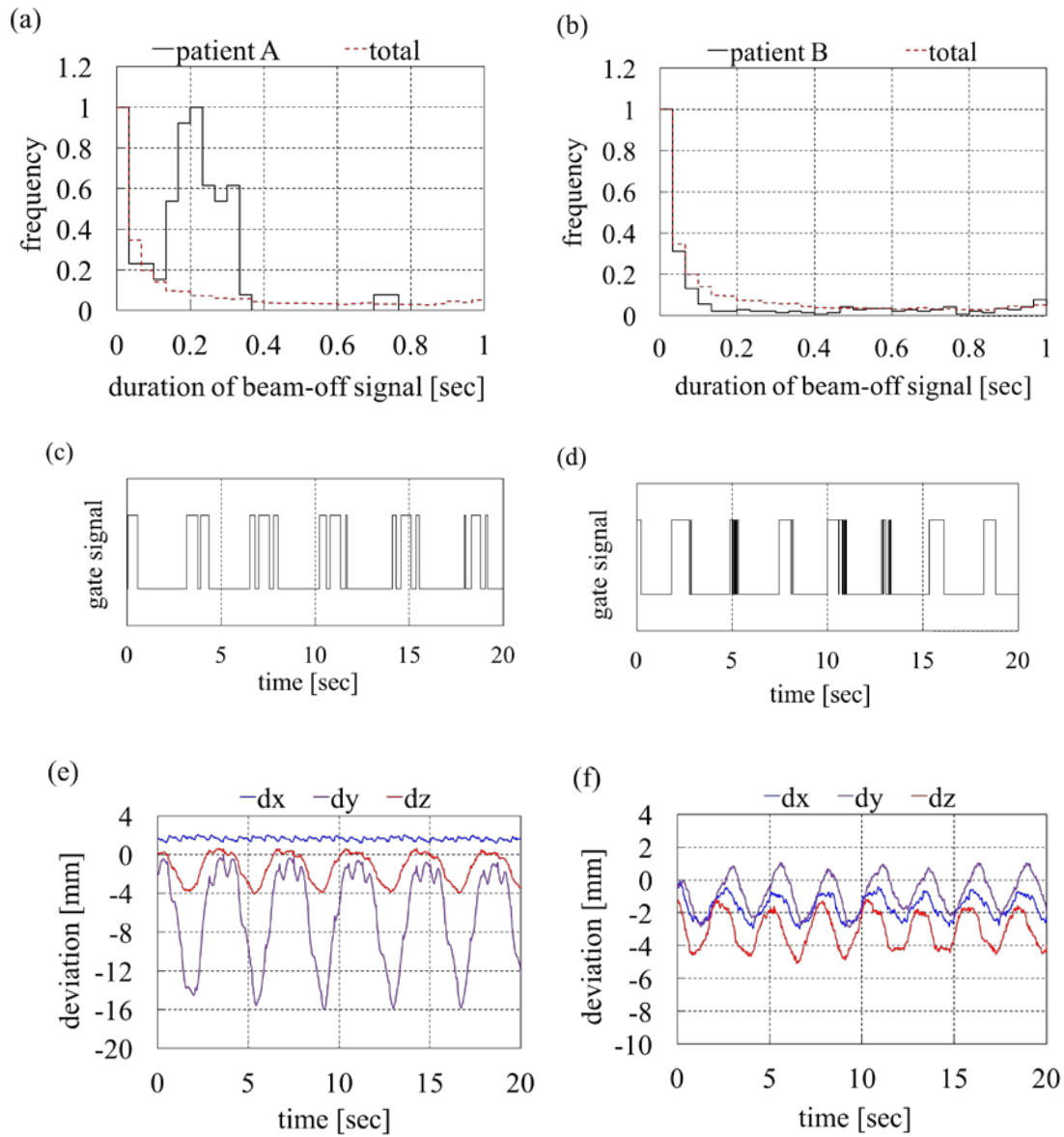


Fig. 6. Examples of normalized frequency histograms of gate-off times for (a) Patient A and (b) Patient B. Dashed and solid lines represent the histograms of the overall gate-off times in the complete dataset (271 datasets) and for each patient, respectively. Portions of the time-series data of the gate signals for (c) Patient A and (d) Patient B. Corresponding marker traces for (e) Patient A and (f) Patient B with a  $\pm 2$  mm gating window.

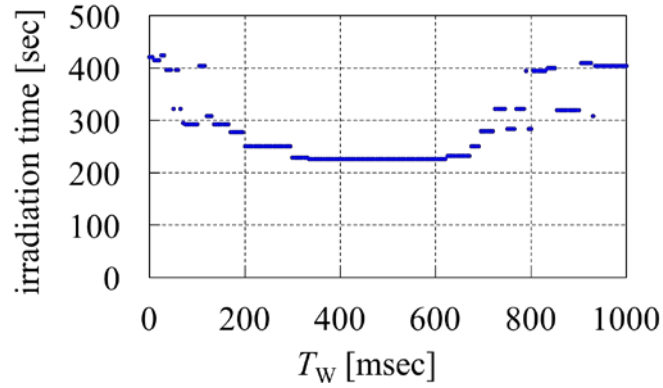


Figure 7. Estimated treatment time for the hepatic tumor patient as a function of  $T_w$ . The dose in this treatment field was 4.48 GyE.

## Discussion

The actual treatment time of the hepatic tumor patient was 250 s, which was shorter than the expected treatment time of 420 s without the multiple gated-irradiation function for the same dose (4.48 GyE). Multiple gated irradiation reduced the treatment time to 59.5% of its nominal value (250 s/420 s). However, the treatment time depends on the treatment planning parameters; that is, the number of spots per layer, number of energy layers, and other parameters. Total irradiation time will be evaluated in a future study by accumulating the treatment data. We also found that the optimal waiting time  $T_w$  in multiple gated irradiation depends on the patient. These differences are attributed to anatomical differences in the tumor positions. For instance, when the fiducial marker is located near the heart, the gate signals will vary under both respiratory and cardiac cycles. Ease of marker recognition will also affect the optimal  $T_w$  value on a patient-by-patient basis; for example, the recognition error of the marker located in a thick region could be large. Hence,  $T_w$  should ideally be optimized for each patient rather than fixed at 0.2 s. In the hepatic tumor patient, the optimum  $T_w$  value was thought to be around 0.4 s rather than 0.2 s (Fig. 7). By setting  $T_w$  to 0.4 s in this patient, the treatment time could be further reduced to 53.8% (226 s/420 s) of the time taken for an ordinary synchrotron operation. The clinical benefits of individually optimizing  $T_w$  should be evaluated in a future study.

There are several possible pitfalls in the current analysis. The pattern of the gate signals depends on the uncertainty of the patient setup. In addition, internal tumor motion includes interfractional variation [27]. Here, we ignored the baseline shift/drift during the therapeutic beam delivery, which also depends on the tumor motion [23] and consequently changes the gate signal patterns and the system efficiency. These biases may be significant but cannot be compensated by the multiple gated-irradiation function. Therefore, the baseline shift/drift should be carefully corrected by patient re-setup during treatment.

To improve the gated-irradiation efficiency, we could reduce the number of frequent gate signal changes in the real-time imaging equipment. For example, large marker recognition errors during low dose imaging can be reduced by image processing techniques [24,28]. The dynamic gating window technique [26] or management of the baseline shift [29] might also compensate for the variation of tumor motion and reduce toggling of the gate signals.

## **Conclusions**

In this study, the gated-irradiation efficiency was evaluated at different  $T_w$  values in order to find the optimum parameter. The highest mean efficiency of gated irradiation was obtained at  $T_w = 0.2$  s. The mean irradiation efficiency was improved by approximately 21% over ordinary synchrotron operation. By applying multiple gated irradiation with  $T_w = 0.2$  s, the irradiation efficiency was improved in 154 (57%) of the 271 cases. We suggest that the multiple gated-irradiation function has potential to improve the gated irradiation efficiency and to reduce the treatment time.

## **Acknowledgments**

This research was supported in part by the Sapporo Health Innovation ‘Smart-H’ project and ‘Global Institution for Collaborative Research and Education (GI-CoRE), Hokkaido University’ of the Ministry of Education, Culture, Sports, Science, and Technology of Japan. The RGPT system was developed by Funding Program for World-Leading Innovative R&D on Science and Technology

(FIRST Program), initiated by the Council for Science and Technology Policy (CSTP). One of the co-authors (Shirato, H.) has received research funds from Hitachi Ltd., Mitsubishi Heavy Industries Ltd., and Shimadzu Corporation.

## References

- [1] Phillips M H, Pedroni E, Blattmann H, Boehringer T, Coray A, Scheib S. Effects of respiratory motion on dose uniformity with a charged particle scanning method. *Phys Med Biol* 1992;37:223–34.
- [2] Bert C, Grozinger S O, Rietzel E. Quantification of interplay effects of scanned particle beams and moving targets. *Phys Med Biol* 2008;53:2253–2265
- [3] Grassberger C, Dowdell S, Lomax A, Sharp G, Shackleford J, Choi N, Willers H, Paganetti H. Motion interplay as a function of patient parameters and spot size in spot scanning proton therapy for lung cancer. *Int J Radiat Oncol Biol Phys* 2013;86:380–386
- [4] Knopf A, Nill S, Yohannes I, Graeff C, et al. Challenges of radiotherapy: report on the 4D treatment planning workshop 2013. *Phys Med* 2014;30:809–815
- [5] Shirato H, Shimizu S, Shimizu T, Nishioka T, Miyasaka K. Real-time tumour-tracking radiotherapy. *Lancet* 1999;353:1331–1332
- [6] Wagman R, Yorke E, Ford E, Giraud P, Mageras G, Minsky B, Rosenzweig K. Respiratory gating for liver tumors: use in dose escalation. *Int J Radiat Oncol Biol Phys* 2003;55:659–668
- [7] Jang S, Huh G, Park S, Yang P, Cho E. The impact of respiratory gating on lung dosimetry in stereotactic body radiotherapy for lung cancer. *Phys Med* 2014;30:682–689
- [8] Kamino Y, Takayama K, Kokubo M, Narita Y, Hirai E, Kawada N, Mizowaki T, Nagata Y, Nishidai T, Hiraoka M. Development of a four-dimensional image-guided radiotherapy system

- with a gimbaled x-ray head. *Int J Radiat Oncol Biol Phys* 2006;66:271–278
- [9] Hoogeman M, Prevost J B, Nuyttens J, Poll J, Levendag P, Heijmen B. Clinical accuracy of the respiratory tumor tracking system of the cyberknife: assessment by analysis of log files. *Int J Radiat Oncol Biol Phys* 2009;74:297–303
- [10] Tsunashima Y, Vedam S, Dong L, Umezawa M, Balter P, Smith A, Mohan R. The precision of respiratory-gated delivery of synchrotron-based pulsed beam proton therapy. *Phys Med Biol* 2010;55:7638–7647
- [11] Minohara S, Kanai T, Endo M, Noda K, Kanazawa M. Respiratory gated irradiation system for heavy-ion radiotherapy. *Int J Radiat Oncol Biol Phys* 2000;47:1097–1103
- [12] Bert C, Gemmel A, Saito N, Rietzel E. Gated irradiation with scanned particle beams. *Int J Radiat Oncol Biol Phys* 2009;73:1270–1275
- [13] Bert C, Saito N, Schmidt A, Chaudhri N, Schardt D, Rietzel E. Target motion tracking with a scanned particle beam. *Med Phys* 2007;34:4768–4671
- [14] Grozinger S O, Bert C, Haberer T, Kraft G, Rietzel E. Motion compensation with a scanned ion beam: a technical feasibility study. *Radiat Oncol* 2008;3:34
- [15] Berbeco R I, Nishioka S, Shirato H, Chen G T, Jiang S B. Residual motion of lung tumours in gated radiotherapy with external respiratory surrogates. *Phys Med Biol* 2005;50:3655–67
- [16] Iwata Y, Kadowaki T, Uchiyama H, et al. Multiple-energy operation with extended flattops at HIMAC. *Nucl Instru Meth Phys Res A*. 2010;624(1):33–38.
- [17] Mori S, Inaniwa T, Furukawa T, Zenklusen S, Shirai T, Noda K. Effects of a difference in respiratory cycle between treatment planning and irradiation for phase-controlled rescanning and carbon pencil beam scanning. *Br J Radiol* 2013;86:20130163

- [18] Seppenwoolde Y, Shirato H, Kitamura K, Shimizu S, Herk M V, Lebesque J V, Miyasaka K. Precise and real-time measurement of 3D tumor motion in lung due to breathing and heartbeat, measured during radiotherapy. *Int J Radiat Oncol Biol Phys* 2002;53:822–834
- [19] Miyamoto N, Ishikawa M, Sutherland K, Suzuki R, Matsuura T, Toramatsh C, Takao S, Nihongi H, Shimizu S, Umegaki K, Shirato H. A motion-compensated image filter for low-dose fluoroscopy in a real-time tumor-tracking radiotherapy system. *J Radiat Res* 2015;56:186–196
- [20] Matsuura T, Miyamoto N, Shimizu S, Fujii Y, Umezawa M, Takao S, Nihongi H, Toramatsu C, Sutherland K, Suzuki R, Ishikawa M, Kinoshita R, Maeda M, Umegaki K, Shirato H. Integration of a real-time tumor monitoring system into gated proton spot-scanning beam therapy: An initial phantom study using patient tumor trajectory data. *Med Phys* 2013;40:071729
- [21] Tsunashima Y, Vedam S, Dong S, Umezawa M, Sakae T, Bues M, Balter P, Smith A, Mohan R. Efficiency of respiratory-gated delivery of synchrotron-based pulsed proton irradiation. *Phys Med Biol* 2008;53:1947–1959
- [22] Shirato H, Onimaru R, Ishikawa M, Kaneko J, Takeshima T, Mochizuki K, Shimizu S, Umegaki K. Real-time 4-D radiotherapy for lung cancer. *Cancer Sci* 2014;103:1-6
- [23] Shimizu S, Miyamoto N, Matsuura T, Fujii Y, Umezawa M, Umegaki K, Hiramoto K, Shirato H. A Proton beam therapy system dedicated to spot-scanning increases accuracy with moving tumors by real-time imaging and gating reduces equipment size. *PLOS ONE* 2014;9:e94971
- [24] Shimizu S, Matsuura T, Umezawa M, Hiramoto K, Miyamoto N, Umegaki K, Shirato H. Preliminary analysis for integration of spot-scanning proton beam therapy and real-time imaging and gating. *Phys Med* 2014;30:555–558
- [25] Umezawa M, Fujimoto R, Umekawa T, Fujii Y, Takayanagi T, Ebina F, Aoki T, Nagamine Y, Matsuda K, Hiramoto K, Matsuura T, Miyamoto N, Nihongi H, Umegaki K, Shirato H.

Development of the compact proton beam therapy system dedicated to spot scanning with real-time tumor-tracking technology. *AIP Conf. Proc.* 2012;1525:360–363

[26] Pepin E W, Wu H, Shirato H. Dynamic gating window for compensation of baseline shift in respiratory-gated radiation therapy. *Med Phys* 2011;38:1912–1918

[27] Shirato H, Suzuki K, Sharp G, Fujita K, Onimaru R, Fujino M, Kato N, Osaka Y, Kinoshita R, Taguchi H, Onodera S, Miyasaka K. Speed and amplitude of lung tumor motion precisely detected in four-dimensional setup and in real-time tumor-tracking radiotherapy. *Int J Radiat Oncol Biol Phys* 2006;64:1229–1236

[28] Wang J, Zhu L, Xing L. Noise reduction in low-dose x-ray fluoroscopy for image-guided radiation therapy. *Int J Radiat Oncol Biol Phys* 2009;74:637–643

[29] Tachibana H, Kitamura N, Ito Y, Kawai D, Nakajima M. Management of the baseline shift using a new and simple method for respiratory-gated radiation therapy: Detectability and effectiveness of a flexible monitoring system. *Med Phys* 2011;38:3971–3980